

# DESIGN CONSIDERATIONS FOR MASK PROJECTION MICROSTEREOLITHOGRAPHY SYSTEMS

Phillip M. Lambert, Earl A. Campaigne III, and Christopher B. Williams  
Design, Research, and Education for Additive Manufacturing Systems Laboratory  
Department of Mechanical Engineering  
Virginia Polytechnic Institute and State University

## Abstract

Mask projection microstereolithography (MP $\mu$ SL) uses a dynamic mask and focusing optics to digitally pattern UV light and selectively cure entire layers of photopolymer resin. These systems have been shown to be capable of creating parts with features smaller than 10 $\mu$ m. In this paper, the authors analyze existing MP $\mu$ SL systems using functional decomposition. Within the context of a morphological matrix, these systems' design embodiment decisions are compared and the resulting performance tradeoffs are quantified. These embodiment decisions include the dynamic mask, UV light source, projection orientation, and supporting optics. The aim of this work is to provide a design guide for the realization of future MP $\mu$ SL systems.

**Keywords:** mask projection, microstereolithography, stereolithography, vat polymerization, morphological matrix, functional decomposition, system design, system analysis, literature review

## 1. Background and Motivation

Within the realm of Additive Manufacturing (AM), stereolithography (SL) is a well-established technology used to create parts, with features as small as 75 $\mu$ m, by crosslinking layers of photopolymer resin with a scanning ultraviolet (UV) laser beam. Mask projection microstereolithography (MP $\mu$ SL) modifies the SL process by replacing the scanning UV laser with a UV light source and dynamic pattern generator (or dynamic mask) to digitally pattern light and expose an entire cross-sectional layer at once. Unlike traditional SL processes, MP $\mu$ SL is not limited by the laser beam radius or its scan speed, and thus enables the creation of feature sizes smaller than 10 $\mu$ m while also reducing build times by an order of magnitude [1–14].

In 1995 Arnaud Bertsch presented the first MP $\mu$ SL system, which he then called integral stereolithography [1], [2], [15]. The general mask projection micro-stereolithography process flow is illustrated in Figure 1. Light is first created by a source - commonly a light emitting diode (LED), lamp, or laser. This light is then conditioned by a series of optics that may include collimating lenses, wavelength filters, and homogenizing rods. A mirror is often used to reflect light onto a dynamic pattern generator (dynamic mask), such that it is parallel to the projection surface. The dynamic pattern generator digitally patterns and projects the incident light as an image. Finally, the patterned light is resized by an optical lens, or series of lenses, to focus the final image on the surface of liquid photopolymer resin. The projected pattern initiates the crosslinking of monomers within the photopolymer resin, causing it to change phases from a liquid to a solid in a process called polymerization.

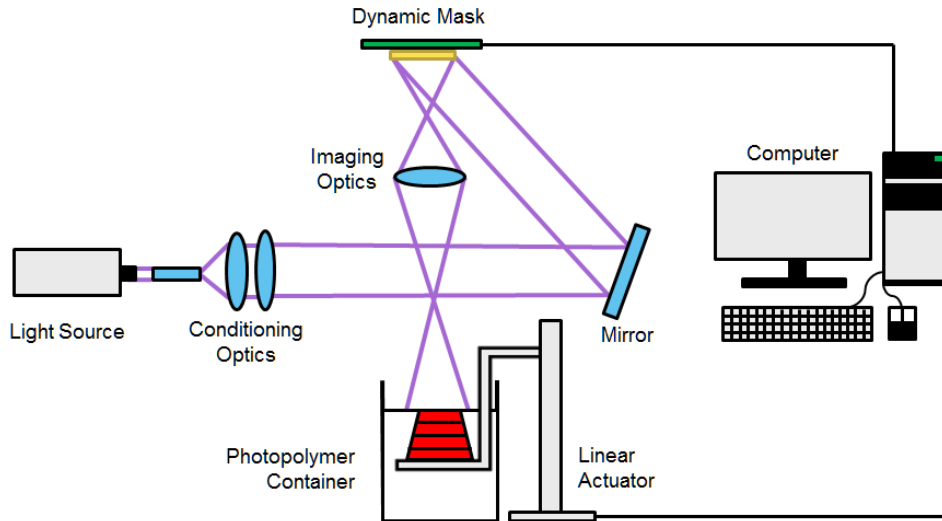


**Figure 1.** Diagram of a typical MμSL system. Purple lines highlight the travel of light.

The first layer of photopolymer resin is cured on a build platform. The build platform is then repositioned such that additional resin recoats the previously cured photopolymer to provide material for creating a subsequent layer. An image of the next cross-sectional layer is projected to cure it on top of the previous layer. After the final cross-section is projected, the completed part is removed and post-processed.

Many MμSL systems have been developed, each providing the same fundamental system functionalities, but with different system embodiments to meet the requirements of a variety of applications (Section 4). This paper analyzes these past MμSL systems and abstracts the inherent system tradeoffs in order to provide readers with a guide for designing future systems and applications. The MμSL process is described in terms of functional components and design considerations in Section 2. Following the AM classification approach suggested by Williams, Rosen and Mistree [16], a morphological matrix design tool is used to visually categorize MμSL design solutions. Performance tradeoffs are identified between the various system components that reoccur throughout published MμSL systems in Section 3. The performance metrics used to quantify these tradeoffs are the systems' (i) achievable layer thickness, (ii) minimum feature size, (iii) build volume, and (iv) vertical build time. Within the organizational context of the presented morphological matrix, this paper categorizes many MμSL systems in Section 4, while drawing conclusions from their design decisions. The results and conclusions of this review are presented in Section 5.

## 2. MP $\mu$ SL Functional Analysis

This section describes the MP $\mu$ SL process as a set of subfunctions and performance parameters, which are shown through a functional decomposition and a morphological matrix.

### 2.1 MP $\mu$ SL System Subfunctions

The MP $\mu$ SL process can be discretized into a set of functional subsystems, each with their own set of unique design considerations. The final performance of a MP $\mu$ SL system is dependent on the sum of these functional parts. They are as follows:

- *Light source* produces the luminous energy that is projected onto the resin surface to selectively cure photopolymer.
- *Conditioning optics* change properties of the projected light for MP $\mu$ SL applications.
- *Dynamic mask* digitally patterns and projects incident light to selectively cure photopolymer.
- *Projection orientation* is the position of the dynamic mask relative to the polymer container.
- *Imaging optics* expand or reduce the projected image to achieve the desired image resolution.
- *Recoat method* supplies liquid photopolymer over previous layers for the creation of new layers.
- *Build platform* supports the object being made.
- *Vertical actuator* repositions the build platform for the creation of new layers.
- *System controls* programmatically alter system properties during the fabrication process.
- *Photopolymer container* holds the reservoir of photopolymer and contains the build platform.
- *Photopolymer* is the raw material used in MP $\mu$ SL to fabricate three dimensional objects.

These subfunctions, and their respective design considerations, are presented as a functional decomposition in Figure 2. This list includes the core system functionalities of MP $\mu$ SL systems; however, it is not necessarily comprehensive. Some applications may require application-specific considerations, such as humidity control or gas metering within an enclosed build volume to reduce the influence of environmental inconsistencies [7].

This discretization of the MP $\mu$ SL process into a set of necessary functional subsystems enables the categorization and comparison of MP $\mu$ SL systems. A morphological matrix – a design tool that presents system subfunctions and their respective potential design solutions – is provided for the MP $\mu$ SL process in Figure 3. Using this tool, a designer is able to create different MP $\mu$ SL embodiments by implementing unique combinations of subfunctions. In addition, this tool can be used as a framework for categorizing and comparing existing MP $\mu$ SL systems on a functional basis.

It is important to note that the presented matrix features only those subfunctions that have the most direct effect on overall system performance. The remaining subfunctions (build platform, vertical actuator, system controls, and photopolymer) are not detailed in this work as they either have only indirect effects on system performance, are common engineering components, and/or are not within the scope of this paper (e.g., controls and materials issues).

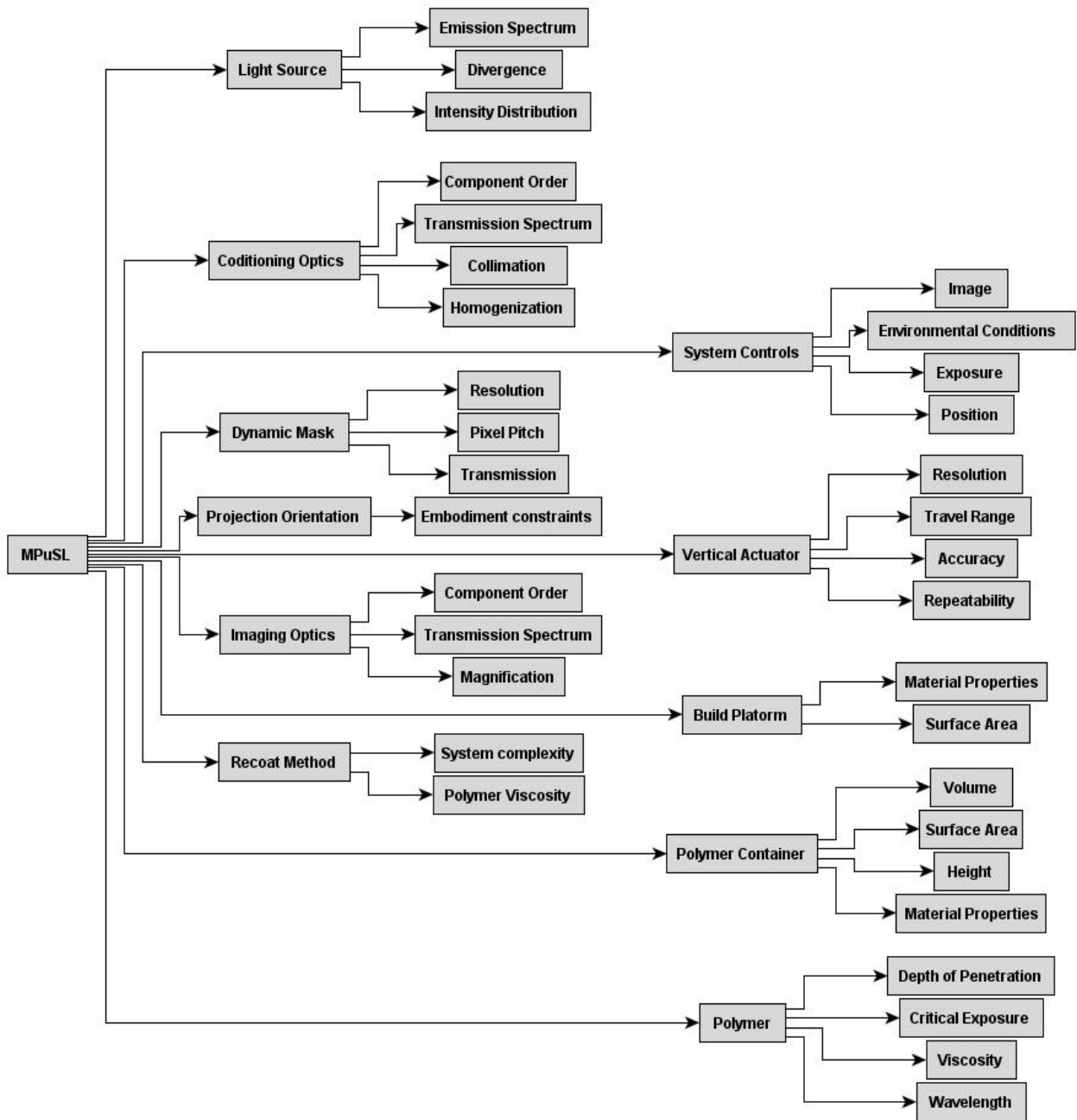


**Figure 2.** Functional decomposition of the MPuSL process relating subfunctions to design considerations

<i>Sub-functions</i>	<i>Solutions</i>			
<b>Light Source</b>	Lamp	Light Emitting Diode (LED)		Laser
<b>Conditioning Optics</b>	Homogenization	Collimation	Filtering	Beam Expansion
<b>Pattern Light</b>	Liquid Crystal Display (LCD)	Digital Micromirror Device (DMD, DLP Projector)		Liquid Crystal on Silicone (LCoS)
<b>Projection Orientation</b>	From Above		From Below	
<b>Imaging Optics</b>	Image Expansion		Image Reduction	
<b>Recoat Method</b>	By gravity	By spreading	By pumping	By dipping

**Figure 3.** Morphological matrix discretizing the MP $\mu$ SL process into a set of functional subsystems and their solutions.

## 2.2 MP $\mu$ SL Performance Parameters

As they share the same broad design goals, all MP $\mu$ SL systems can be evaluated via a common set of design metrics, and thus provide a basis for comparison. The MP $\mu$ SL performance parameters and relationships are as follows:

- *Layer thickness* ( $\mu\text{m}$ ) is a metric for quantifying vertical (z-axis) resolution. The achievable layer thickness is largely determined by the employed recoating method, actuator resolution, polymer characteristics, and projection orientation.
- *Minimum feature size* ( $\mu\text{m}$ ) defines the cross-sectional resolution and smallest obtainable features in the X-Y plane. The dynamic pattern generator, projection orientation, and imaging optics define the projected cross-sectional resolution, while the recoating method restricts the physical minimum feature size.
- *Build volume* ( $\text{mm}^3$ ) is a metric for quantifying the dimensions of the largest printed part. The dynamic mask and imaging optics limit the size of the projected image in the X-Y plane and thus the maximum build volume.
- *Vertical build rate* ( $\text{mm/s}$ ) is a metric that quantifies process throughput. Unfortunately, MP $\mu$ SL build rates are often published using unclear terms. For example, many authors state throughput in units of seconds per layer, but do not specify whether this is the exposure time per layer or total build time per layer. This is compounded by the fact that each system uses different photopolymers, which require different exposures. This often prevents the direct comparison of vertical build rates for previously published work.

A Process Planning matrix (from Quality Function Deployment methodology) is used to illustrate the interrelationships between subfunctions and performance metrics (Table 1). The strength of each relationship is indicated by assigned values where 1 represents a weak relationship, 3 a medium relationship, and 9 a strong relationship. For example: There is a strong relationship (9) between the minimum feature size ( $\mu\text{m}$ ) and imaging optics of a MP $\mu$ SL

machine, because the imaging optics expand or reduce the projected features. In addition, build rate is primarily determined by projection orientation and recoating method.

**Table 1.** QFD Process Planning matrix illustrating the interrelationships between MP $\mu$ SL functional subsystems and performance parameters.

	Minimum Feature Size ( $\mu\text{m}$ )	Layer Thickness ( $\mu\text{m}$ )	Build Volume ( $\text{mm}^3$ )	Vertical Build Time ( $\text{mm/s}$ )
<b>Light Source</b>	1			3
<b>Conditioning Optics</b>	1			1
<b>Pattern Light</b>	9		9	
<b>Projection Orientation</b>	9	1		9
<b>Imaging Optics</b>	9		9	
<b>Recoat Method</b>	9	3		9

### 3. MP $\mu$ SL System Components

In this section, the authors analyze possible solutions to the MP $\mu$ SL subfunctions presented in Figure 3 and Table 1. The design considerations (Figure 2) for each solution are also detailed.

#### 3.1 Light Source

There are three performance criteria that are particularly important for selecting a light source for MP $\mu$ SL applications:

- The *emission spectrum* of the light source must include the wavelength required by the selected photopolymer to achieve photopolymerization.
- The *intensity of light* at that wavelength must be great enough to reach the photopolymer's critical exposure in a reasonable amount of time (e.g., < 60 seconds). This is a key factor in determining system build speed.
- The *divergence* and *intensity profile* of light determine the conditioning and imaging optics required to generate a focused image of homogenous intensity.

Lamp-based light sources reflect light emitted in all directions from a bulb into a light guide. These lamps output high intensity, broad-spectrum light often ranging between 350nm and 500nm. For this reason, lamp light sources are compatible with a wide variety of photopolymer resins of different wavelength sensitivities. Lamp-based light sources are the most commonly used light source for exposing photopolymers in MP $\mu$ SL systems [4–9], [14], [17–24].

Light Emitting Diode (LED) sources are also used in MP $\mu$ SL systems [3]. In general, LED sources have longer operating lives, lower cost, smaller package size, and lower heat generation than mercury lamps and lasers. LED sources generally output lower light intensities than lamps at one or more wavelengths, which may be chosen to match the photopolymer's polymerization wavelength. LED sources are therefore more energy efficient than mercury lamps and lasers, using energy more efficiently to photopolymerize the same volume of photopolymer [3].

Lasers have also been used in MP $\mu$ SL systems [1], [2], [10–13]. Laser light sources may emit light at a single wavelength or across multiple wavelengths. Lasers are available in ultraviolet, visible, and infrared wavelengths, but often cost thousands of dollars more than the other two light source options.

### 3.2 Conditioning Optics

The system of optical components between the light source and dynamic mask generator is referred to as the conditioning optics (Figure 1). These optical components change the properties of the original light source before reaching the dynamic mask. Unfortunately, published MP $\mu$ SL systems underreport the specifics of these optical components, so it is difficult to discuss them in great detail. However, commonly mentioned components include:

- *Homogenizing rods* that internally reflect light repeatedly to create even intensity profiles. Light without a homogenous intensity profile fabricates inconsistent layer thicknesses along the projected image. These inconsistencies will compound and create dimensionally inaccurate parts [5], [24].
- *Collimating lenses* may be used to collimate a highly diverging source such as a lamp. Well collimated light diverges very little, preventing unwanted beam divergence and the resulting decrease in light density [4], [6–9], [17], [18], [23], [25].
- *Filters* may be used to remove unwanted wavelengths, isolating the desired wavelength [4], [6–9], [17], [18], [23], [25].
- *Beam expanding optics* may be used to expand already collimated light from an LED, laser, or collimating lenses [1], [2], [10–14].

Different light sources produce different levels of collimation and homogeneity. Lasers produce the most collimated light with the most homogenous light intensity. Lamp light sources often possess a Gaussian intensity distribution and non-collimated, widely diverging light. It is the authors' experience that LED light sources are often less collimated than lasers and possess periodic drops in intensity distributions originating from their diodes.

Using the optical components listed above, the collimation and homogeneity of lamp and LED light sources can be improved; however, it is difficult to achieve the same level of performance as a laser.

### 3.3 Pattern Light

A dynamic pattern generator digitally patterns and projects the conditioned light. Dynamic masks all operate by discretizing light over a 2D array of pixels, each individually controlling the light's path. Important design considerations of the dynamic mask include its resolution, pixel pitch, and transmission. Dynamic masks are used primarily in the digital display industry and

come in standard resolutions (e.g., 800x600, 1024x768, and 1920x1080). The pixel pitch represents the size of each pixel and the space between pixels. Because optical magnification must be uniform, the resolution and pixel pitch determines the ratio between the projected image area and the minimum feature size. This limitation can only be overcome by moving the mask in relation to the build platform, such that images are stitched together in the photopolymer [4]. Digital Micromirror Device (DMD), Liquid Crystal Display (LCD), and Liquid Crystal on Silicon (LCoS) technologies have been used as dynamic masks throughout MP $\mu$ SL.

### 3.3.1 Liquid Crystal Display (LCD)

Early MP $\mu$ SL systems were implemented using LCD devices as the dynamic mask [1], [2], [10–14]. LCD chips digitally pattern light by switching pixels between opaque and transparent states, achieved by controlling the orientation of the liquid crystal molecules comprising the pixel. However, the original LCD devices were not designed for use with UV light, and only transmit about 12.5% of UV light [5].

### 3.3.2 Digital Micromirror Device (DMD)

Given LCD's limited UV transmission, the DMD was used almost exclusively in MP $\mu$ SL systems after 1999 [4–10], [17–21], [23–26]. DMD's discretize light over a 2D array of aluminum micromirrors that are individually actuated between on and off orientations ( $\pm 12$  degrees) by electrostatic forces applied at their hinges. The DMD offers many advantages when compared to other available dynamic masks:

- The DMD has small pixel sizes and narrow gaps between pixels. Because of this, DMDs are designed with greater pixel density and can reflect incident light with a more uniform intensity (less light is lost in the gaps). Therefore DMDs have a higher filling ratio (reflective area/total area) compared to LCDs: 91% versus 57% [5].
- The modulation speed between states for individual pixels is also much less for DMDs as compared with LCDs: 20 $\mu$ s versus 20ms. This allows for greater control of exposure time and an increased ability to modulate individual pixels as to achieve gradient, grayscale projection and digitally modulate the intensity of reflected light [5].
- The mirrors of the DMD are surfaced with aluminum that reflects approximately 88% of the incident light, while LCDs typically transmit only 12.5% of incident light. DMDs are therefore more efficient at patterning light and require less powerful light sources, reducing system cost and complexity [5].

### 3.3.3 Liquid Crystal on Silicone (LCoS)

Liquid Crystal on Silicone (LCoS) devices are a reflective version of LCD technologies. LCoS chips possess a 2D array of liquid crystals between one transparent thin-film transistor (TFT) and one silicon semiconductor. The transparency of each pixel is controlled by the applied voltage just as in LCD chips. Unlike LCD, the opaque pixels pass light to the underlying reflective coating to project a pattern. Blocked light is reflected in a different direction. Unlike a DMD, the reflective surface is static while the liquid crystals determine the reflection of light [3].

LCoS devices possess many of the same advantages over LCD devices as DMD devices. LCoS devices generally have higher fill rates and smoother reflective surfaces than the DMD. Unfortunately LCoS chips have poor contrast ratios and do not produce deep blacks. In

M $\mu$ SLA, projected images will have a base level of intensity even in areas that are meant to be absent of light. This may unintentionally cure photopolymer and may even encourage the development of artifacts or otherwise restrict dimensional accuracy within the cross section. Furthermore, LCoS chips are difficult and expensive to manufacture making their availability and cost to performance ratio less than that of DMDs [27].

### 3.4 Imaging Optics

The optical components that modify the projected image are regarded as the imaging optics. This series of lenses is typically designed with the intention of capturing the light projection transmitting from the pattern generator and focusing it on the build surface. By choosing lenses with specific focal lengths and numerical apertures, a desirable reduction ratio can be achieved.

The reduction ratio is what determines the achievable resolution and working area, but there is a tradeoff between the two characteristics. A higher reduction ratio (lower magnification) means that higher resolutions are achievable, but this reduces the overall projection area and results in smaller part sizes. System magnification can be calculated using lens equations. For example, Choi explains for a system with a magnification of 0.434, one pixel on the DMD (pitch of 13.68  $\mu\text{m}$ ) would reduce to approximately 5.9  $\mu\text{m}$  on the resin surface [17]. This constitutes the physical limit of the X-Y resolution of a system, provided that the recoat method or print orientation does not inhibit achievable feature sizes.

### 3.5 Recoat

There are several methods for reapplying resin to the build surface. The methods include recoating by gravity, by spreading, by pumping and by dipping (Figure 3).

Recoat by dipping is the most commonly used method for recoating in microstereolithography. In this method, the build platform is dipped below the resin surface to exactly one layer thickness depth. That layer is cured, and the stage descends into the vat of photopolymer, which allows for fresh uncured resin to flow over the previously created layer. The stage then returns to a location where the previously cured layer is exactly one layer thickness below the resin surface [4–8], [17–20].

Recoat by gravity is used exclusively in bottom-up projection systems (explained further in section 3.6). Unlike the dipping process when projecting from above, the build platform is raised by the z-axis actuator to create a gap between the platform and the resin container for the next layer. If the photopolymer has a low viscosity, it will flow into the created gap. If the photopolymer has a high viscosity, the platform needs to be raised to an exaggerated height such that the photopolymer can fill the gap. The z-axis actuator then moves the platform down until the desired layer thickness gap is achieved, while extra photopolymer is forced to the sides [26]. Hypothetically, pumping the resin into the created gap could assist the recoat process when the viscosity is too high.

Recoat by pumping is used rarely and does not refer specifically to a recoat practice. Systems that utilize pumping in the recoat process typically are paired with a dipping process. One instance of pumping identified in literature is a syringe pump that purges uncured resin from the build surface with a high density “filler” material to prepare for the next layer [21]. In a multi-

material system developed by Choi, a “deep dip” process is imitated through precise and extensive pumping [25].

Wiping or spreading uncured resin for recoating is a method common in stereolithography practices [28], but is seldom used in microstereolithography. However, some MP $\mu$ SL systems utilize a squeegee or wiping system to recoat or level the resin surface [22].

### 3.6 Projection Orientation

When deciding upon a base design for a microstereolithography system, besides the dynamic mask, one of the most critical considerations is the orientation in which the system will be projecting light on the build surface. Typically, there are two orientation options as shown in Figure 4: a top-down approach where the path of light is projected from above onto the resin surface (also referred to as “from above” projection orientation) and a bottom-up approach where light is projected through the bottom surface of vat through a transparent window (also referred to as “from below” projection orientation).

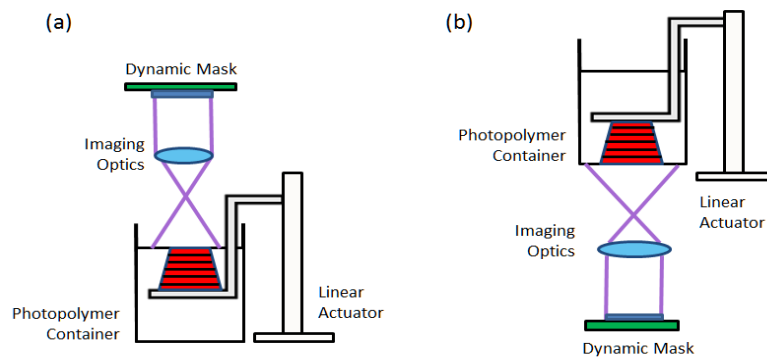


**Figure 4.** Illustration of different projection orientations: (a) image projection from above and (b) image projection from below.

#### 3.6.1 Projecting from above

Typically the slower and more common of the two possible system orientations, projecting from above generally utilizes the dipping method to recoat the part. This approach demands that a designer account for resin characteristics, such as surface tension, viscosity, and wetting, to tune the process and achieve the desired layer thickness. In addition, these characteristics affect polymer settling time, which along with actuator speed, directly influences the process throughput.

In an effort to reduce recoat times, vibration assisted leveling has been experimented with to encourage quicker leveling time of the photopolymer and to obtain thin layers [20], [29]. Also, as mentioned in Section 3.5, Takahashi provides one instance in which a squeegee mechanism is used for adjustment of the resin surface in MP $\mu$ SL [22]. However, as high resolution is generally in the scope of the top-down design, this type of recoat is avoided as sweeping motions may be enough to agitate the resin or catch the part, destroying the print entirely.

### 3.6.2 Projecting from beneath

Projecting images through the bottom of the photopolymer container offers several advantages over projecting images from above the container.

- Less photopolymer is required in the reservoir. Because the build part is not submerged in photopolymer as when projecting from above, the reservoir container is independent of part height and can be shallower. Less photopolymer can save time and/or reduce cost.
- System complexity decreases while the overall vertical print speed increases. When projecting from below, gravity is used to more quickly move and settle the photopolymer. Therefore it is unnecessary to implement recoating mechanisms like squeegees or long waiting periods for photopolymer to settle.
- Thinner layers are theoretically possible. Achievable layer thickness in this orientation is determined by the gap between the previously printed layer and the floor of the container, which is directly limited and controlled by the resolution of the vertical actuator of the build platform.
- Photopolymer can polymerize faster because it is removed from ambient oxygen that would otherwise inhibit crosslinking.

As photopolymer cures between the floor of the resin container and the previous layer, it adheres strongly to both. Forces upwards of 50N must be applied to overcome this adhesion and move the build platform, destroying smaller features in the process [26]. Therefore, there is an inherent tradeoff between printing speed and printing resolution for MP $\mu$ SLA machines.

Researchers have developed a peeling process that is used when projecting underneath to alleviate feature destruction caused by separation. In this process either the build tray or resin vat is separated from the other by applying a gradual peeling force (like tape from a table). This process reduces the separation force greatly, preserving features smaller than using the same system without peeling. Unfortunately, the peeling process may prolong total build time and negate the inherent speed advantage. Chen's research group, however, has developed a fast mask projection stereolithography process that bypasses this design tradeoff by applying a flexible silicone membrane to the floor of the resin container [26]. This SYLGARD silicone gel maintains a thin oxidation layer directly on its surface, inhibiting photopolymerization so that a substantially smaller adhesion force is developed. The membrane is also flexible so that the polymer container can slide easily under the build part, to another fresh section of photopolymer (in the same container) for the next layer to cure. This process emulates a peeling step but with much smaller displacements and applied forces, making the impact on overall print speed negligible.

## 4. Categorization and Analysis of MP $\mu$ SL Systems

The morphological matrix introduced in Figure 3 provides a basis on which existing MP $\mu$ SL systems can be analyzed. The existing systems are presented in this section via a categorization based on the critical architectural components of each system. Each morphological matrix is accompanied by a corresponding table that specifies the systems' respective performance parameters. Together, this data provides a basis for determining the effect of system design decisions on critical performance parameters.

#### 4.1 First Generation – LCD MP $\mu$ SL Systems

Bertsch, Chatwin, and Monneret published the first MP $\mu$ SL systems. These systems all use beam expansion for their conditioning optics, LCD masks to pattern light, project images from above the photopolymer, reduce the projected image in size, and recoat photopolymer by dipping. This design architecture is illustrated in Figure 5 using the morphological matrix previously present in Section 2.2, performance parameters are included in Table 2.

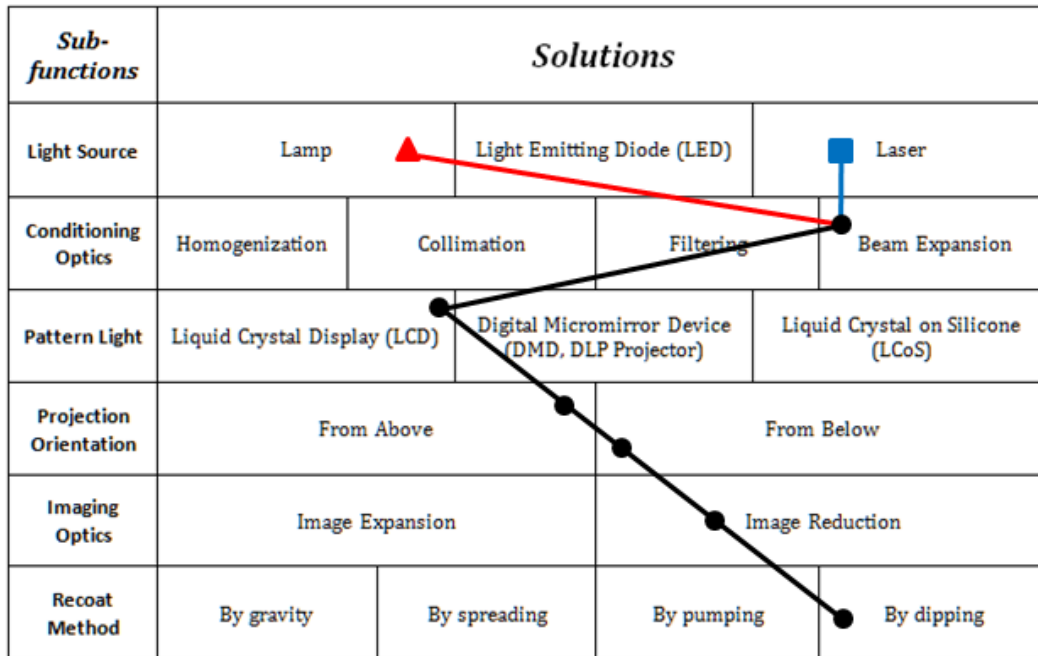


**Figure 5.** Morphological matrix categorizing MP $\mu$ SL machines that use a LCD pattern generator to project images from above the build platform.

**Table 2:** Performance parameters for the MP $\mu$ SL systems categorized in Figure 5.

	Ref	Research Group	Year	Special Features	Min. Feature Size	Min. Layer Thickness	Maximum Part Size	Vertical Build Rate
■	[1], [2]	Bertsch	1997	LCD,Laser, 515 nm	5 $\mu$ m	5 $\mu$ m	1.3 x 1.3 x 10 mm <sup>3</sup>	110 layers in 90 minutes
■	[10–13]	Chatwin	1998	LCD,Laser, 351.1 nm	5 $\mu$ m	Not reported	50 x 50 x 50 mm <sup>3</sup>	60 second exposure per layer
▲	[14]	Monneret	1999	LCD,Lamp, 530nm	5 $\mu$ m	10 $\mu$ m	3.2 x 2.4 x 1.3 mm <sup>3</sup>	60 layers per hour

All of these machines are capable of producing 5  $\mu$ m minimum feature sizes with layer thicknesses ranging from 5 to 10 $\mu$ m. The machines published by Bertsch and Monneret are particularly noteworthy because they use visible light to cure photopolymer. Future MP $\mu$ SL research moved away from visible photopolymers in favor of curing with UV light. Exposure times for these machines varied, but were roughly 60 seconds per layer on average. The following section introduces second generation MP $\mu$ SL systems.

## 4.2 Second Generation – DMD MP $\mu$ SL Systems

The systems categorized in this section use a DMD to dynamically shape the projected image. These systems were grouped together in order to identify the paradigm shift in design decisions with the advent of the DMD. As outlined in Section 3.3.2, the transition from LCD to DMD was a result of better performance characteristics such as smaller pixel sizes, narrower gaps between pixels, higher modulation speeds, and high reflectivity. The morphological matrix presented in Figure 6 represents systems that utilize a lamp, DMD dynamic mask, from-above projection, image reducing optics, recoat by dipping, but employ unique conditioning optics.

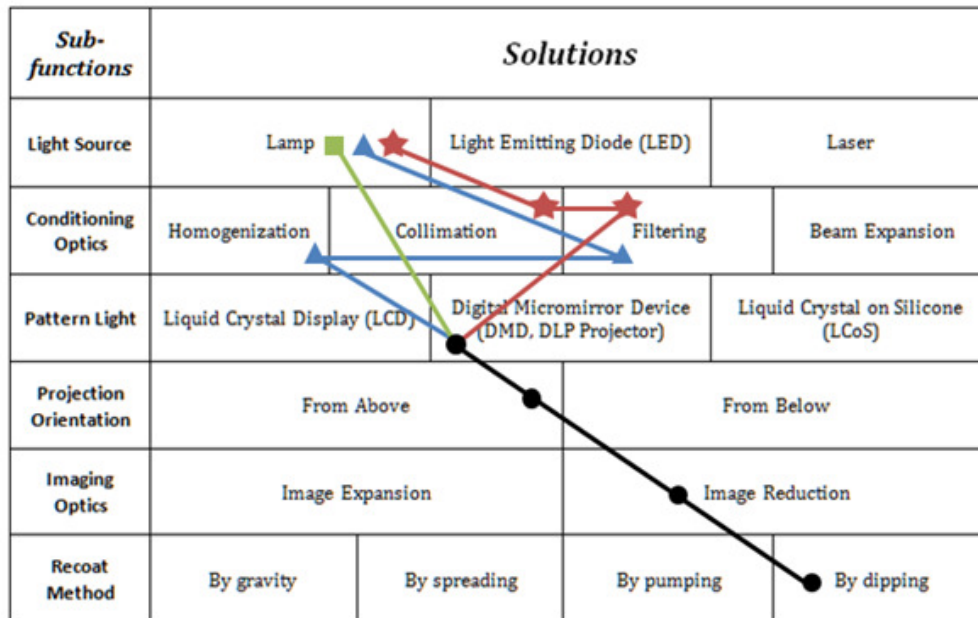


**Figure 6:** Morphological matrix categorizing MP $\mu$ SL machines that use a DMD pattern generator to project images from above the build platform.

**Table 3:** Performance parameters for the MP $\mu$ SL systems categorized in Figure 6.

	Ref	Research Group	Year	Special Feature	Min. Feature Size	Min. Layer Thickness	Part Size	Vertical Build Rate
★	[6]	Rosen	2007	DMD, 365 nm	6 $\mu\text{m}$	400 $\mu\text{m}$	2 x 2 x 1 $\text{mm}^3$	90s per layer
★	[7]	Rosen	2007	DMD, 365, 435, 647 nm	5 $\mu\text{m}$	5 $\mu\text{m}$	not reported	60s per layer
★	[17]	Wicker	2009	DMD, 365 nm	30 $\mu\text{m}$	4 $\mu\text{m}$	1.95 x 1.95 x 2.4 $\text{mm}^3$	<1s per layer
★	[4]	Lee	2008	DMD, 365nm, XY translation	2 $\mu\text{m}$	5 $\mu\text{m}$	10 x 10 x 2.68 $\text{mm}^3$	100s per layer
★	[8], [9]	Bertsch	1999	DMD, visible	5 $\mu\text{m}$	5 $\mu\text{m}$	6 x 8 x 15 $\text{mm}^3$	700 layers in 2.5 hours
★	[18], [23]	Bertsch	2000	DMD, UV	10 $\mu\text{m}$	10 $\mu\text{m}$	10.24 x 7.68 x 20 $\text{mm}^3$	200 layers in 1 hour
▲	[5]	Zhang	2005	DMD, 364 nm, fly-eye lens	0.6 $\mu\text{m}$	5 $\mu\text{m}$	not reported	not reported
■	[19]	Roy	2006	DMD, 355 nm	20 $\mu\text{m}$	150 $\mu\text{m}$	not reported	90s per layer
■	[20]	Hadipoespito	2003	DMD, 365 nm	20 $\mu\text{m}$	100 $\mu\text{m}$	not reported	not reported

As seen in Table 3, the reported achievable feature size of the DMD projection from above systems utilizing the dipping recoat method ranges from 0.6 to 30  $\mu\text{m}$ . While smaller feature sizes were achieved with DMD based systems, the average achievable feature size is not significantly smaller than LCD systems. Unfortunately, the vertical build rate metric for many of these systems are not comparable as many publications use different speed metrics (as discussed in Section 2.3). Regardless, all systems in Figure 5 and Figure 6 use the dipping recoat method, and their build times seem comparable. However, as LCD masks transmit only 12.5% of UV light (as mentioned in Section 3.3.1), build time can increase by a factor of 7 when compared to systems using a DMD with the same light source.

Figure 7 and Table 4 presents systems using a DMD dynamic mask to project images from above, while employing alternative solutions to achieve recoating.

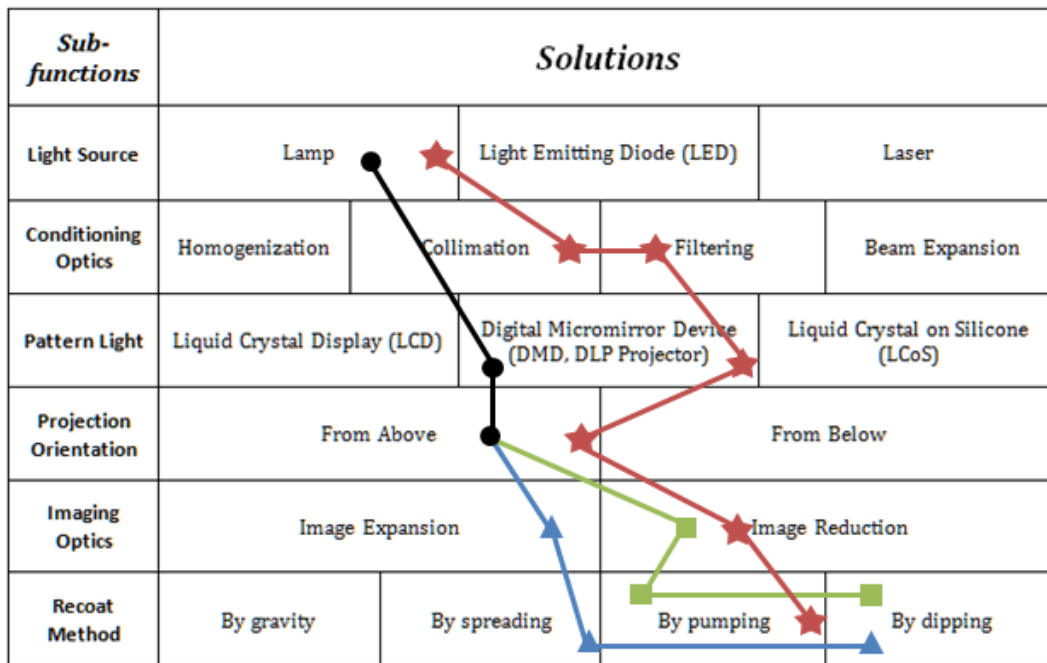


Figure 7: Morphological matrix categorizing MP $\mu$ SL machines that use alternative recoat methods.

Table 4: Performance parameters for the MP $\mu$ SL systems categorized in Figure 7.

	Ref	Research Group	Year	Special Feature	Min. Feature Size	Min. Layer Thickness	Part Size	Vertical Build Rate
★	[25]	Wicker	2009	DMD, 365 nm, multi material	~50 $\mu\text{m}$	21 $\mu\text{m}$	~ 2 x 2 x 4 mm <sup>3</sup>	8-12s per layer
▲	[22]	Takahashi	2000	DMD, 365 nm	50 $\mu\text{m}$	200 $\mu\text{m}$	~ 2 x 2 x 2 mm <sup>3</sup>	not reported
■	[21]	Roy	2008	DMD, 355 nm	50 $\mu\text{m}$	50 $\mu\text{m}$	not reported	60s per layer

Comparing the systems' performances listed in Tables 2 and 3 versus Table 4 (which primarily differ by recoat method) suggests that systems that do not use recoat by dipping generally have larger minimum feature sizes (approximately 50  $\mu\text{m}$ ) and layer thicknesses ranging from 21  $\mu\text{m}$  to 200  $\mu\text{m}$ . This indicates that dipping may be the preferable method for

recoating if the goal of system is to achieve a minimum feature sizes (as discussed in Section 3.5).

### 4.3 Third Generation – From Below Projection

As the embodiment of second generation systems became a standard, some researchers have begun experimenting with alternative projection orientation in the effort to reduce build time. The system architecture presented in Figure 8 and Table 5 is unique as it projects from below and recoats by gravity.

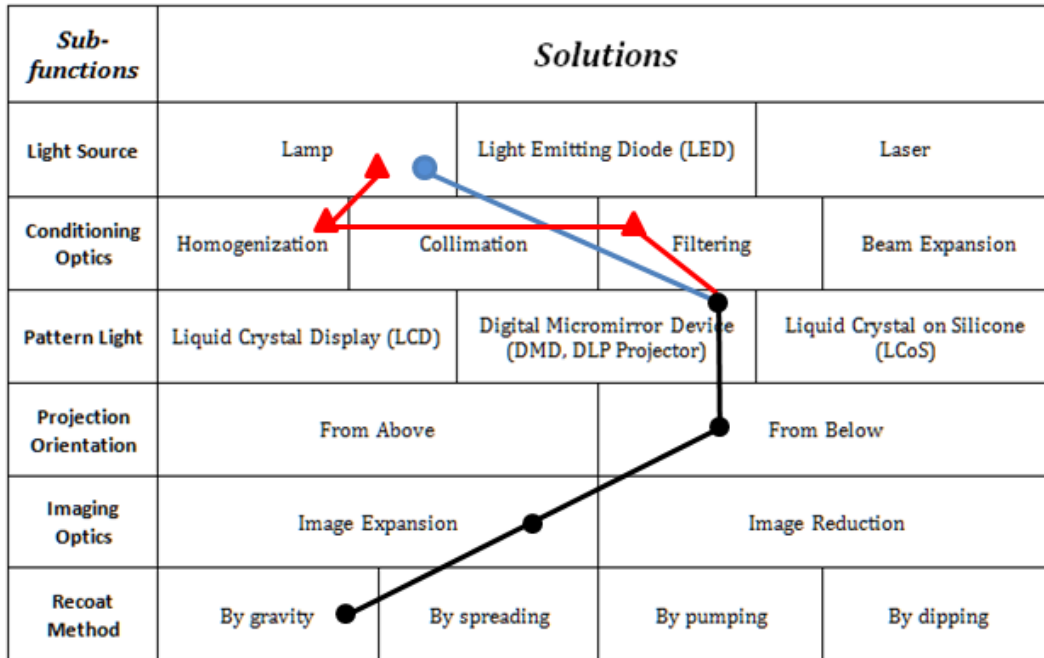


**Figure 8.** Morphological matrix categorizing MP $\mu$ SL machines that use a DMD pattern generator to project images from below the build platform.

**Table 5.** Performance parameters for the MP $\mu$ SL systems categorized in Figure 8.

	Ref	Research Group	Year	Special Features	Min. Feature Size	Min. Layer Thickness	Maximum Part Size	Vertical Build Rate
●	[26]	Chen	2012	DMD, Lamp, visible	400 $\mu$ m	100 $\mu$ m	48 x 36 $\text{mm}^2$	180 mm per hour
▲	[24]	Kang	2012	DMD, Lamp, UV	Not reported	Not reported	14.6 x 10.9 $\text{mm}^2$	Not reported

The feature sizes reported in Table 5 are much larger than those of the systems listed in the Tables 2-4, but the part size is also much larger. The print speed is the quickest of all systems analyzed [26]. This suggests that projecting from below is indeed quicker, but cannot achieve the resolution of top down projection systems. Work in this system embodiment still developing, and there is room for further improvement based on the performance parameters advantages.

#### 4.4 Alternative Embodiments

The last system is unique in that it is the only published system that utilizes an LED light source, and is the only published system that uses a LCoS device to digitally pattern light. Figure 9 and Table 6 outline this system and characterizes its performance.

<i>Sub-functions</i>	<i>Solutions</i>			
Light Source	Lamp	Light Emitting Diode (LED)	Laser	
Conditioning Optics	Homogenization	Collimation	Filtering	Beam Expansion
Pattern Light	Liquid Crystal Display (LCD)	Digital Micromirror Device (DMD, DLP Projector)	Liquid Crystal on Silicone (LCoS)	
Projection Orientation	From Above		From Below	
Imaging Optics	Image Expansion		Image Reduction	
Recoat Method	By gravity	By spreading	By pumping	By dipping

**Figure 9.** Morphological matrix categorizing MP $\mu$ SL machines that use a LCoS pattern generator to project images from above the build platform.

**Table 6.** Performance parameters for the MP $\mu$ SL systems categorized in Figure 9.

	Ref	Research Group	Year	Special Features	Min. Feature Size	Min. Layer Thickness	Maximum Part Size	Vertical Build Rate
■	[3]	Zheng	2012	LCoS, LED, 395nm	1.3 $\mu$ m	10 $\mu$ m	2.56 x 1.44 mm <sup>2</sup>	Not reported

This unique system achieves very small feature sizes, comparable layer thickness and part size of other projection from above, recoat by dipping systems. It follows the trend that high resolution is achievable by combining recoating via dipping with the top-down orientation.

## 5. Closure

This paper presents a MP $\mu$ SL morphological matrix that is designed to functionally categorize and compare the fundamental design decisions solved in the realization of MP $\mu$ SL systems. Using this matrix, several published MP $\mu$ SL systems are analyzed in terms of critical MP $\mu$ SL performance parameters: minimum feature size ( $\mu\text{m}$ ), layer thickness ( $\mu\text{m}$ ), build volume ( $\text{mm}^3$ ), and vertical build time ( $\text{mm/s}$ ). These performance parameters are expressed in units that serve as a standard benchmark to promote direct quantitative comparisons between MP $\mu$ SL systems. From this analysis, relationships between system performance and the corresponding subsystems solutions have been identified to indicate general trends and tradeoffs.

- The most common system embodiments project images from above the photopolymer container and dip the build platform to achieve recoating. These systems are capable of achieving the smallest feature sizes, which are close to 1  $\mu\text{m}$ .
- Dynamic mask selection does not significantly affect the minimum achievable feature size. While pixel pitch is a relevant design consideration, final feature size is ultimately determined by the imaging optics.
- Dynamic mask selection significantly affects the vertical build rate of a MP $\mu$ SL system. LCD masks transmit only 12.5% of UV light, which can increase build time by a factor of 7 when compared to using a DMD with the same light source.
- The relationship between part size and feature size is equivalent to the relationship between aspect ratio and pixel pitch for any dynamic mask. Future dynamic masks with an equivalent pixel pitch but with greater resolution will enable creation of smaller feature sizes on equally sized parts, or the same feature sizes on larger parts.
- If a fast vertical build rate is priority, then system embodiment should project images from below the photopolymer vat. By using a gravity-assisted recoat approach, vertical build rates can be improved by an order of magnitude.
- The type of light source is noncritical provided that emission properties (wavelength and intensity) are suitable, and appropriate light conditioning is performed.

Amongst published MP $\mu$ SL systems, design trends have changed historically. Exploration of novel form factors and embodiments has been limited. An area for future research is in exploring more unique embodiments and subsystem solutions. In doing so, the relationships between MP $\mu$ SL performance parameters and subsystem solutions can be more broadly and quantitatively compared. Ultimately, such relationships could be used to develop processes more optimized for desired performance as governed by the application.

## 6. Acknowledgements

Earl Campaigne is supported by a research assistantship provided by a grant from the Center for Innovative Technology. Philip Lambert is supported by a research assistantship provided by Virginia Tech's Institute for Critical Technology and Applied Science.

## References

- [1] A. Bertsch, S. Zissi, and J. Y. Je, “Microstereophotolithography using a liquid crystal display as dynamic mask-generator,” 1997.
- [2] A. Bertsch and J. C. Andr, “Study of the spatial resolution of a new 3D microfabrication process : the microstereophotolithography using a dynamic mask-generator technique,” vol. 107, pp. 275–281, 1997.
- [3] X. Zheng, J. Deotte, M. P. Alonso, G. R. Farquar, T. H. Weisgraber, S. Gemberling, H. Lee, N. Fang, and C. M. Spadaccini, “Design and optimization of a light-emitting diode projection micro-stereolithography three-dimensional manufacturing system.,” *The Review of scientific instruments*, vol. 83, no. 12, Dec. 2012.
- [4] Y. M. Ha, J. W. Choi, and S. H. Lee, “Mass production of 3-D microstructures using projection microstereolithography,” *Journal of Mechanical Science and Technology*, vol. 22, no. 3, pp. 514–521, May 2008.
- [5] C. Sun, N. Fang, D. M. Wu, and X. Zhang, “Projection micro-stereolithography using digital micro-mirror dynamic mask,” *Sensors and Actuators A: Physical*, vol. 121, no. 1, pp. 113–120, May 2005.
- [6] A. Limaye and D. D. W. Rosen, “Multi-Objective Process Planning Method For Mask Projection Stereolithography,” Georgia Institute of Technology, 2007.
- [7] B. M. Comeau, “Fabrication of Tissue Engineering Scaffolds Using Stereolithography,” no. December, 2007.
- [8] a. Bertsch, H. Lorenz, and P. Renaud, “3D microfabrication by combining microstereolithography and thick resist UV lithography,” *Sensors and Actuators A: Physical*, vol. 73, no. 1–2, pp. 14–23, Mar. 1999.
- [9] A. Bertsch, L. Beluze, and P. Renaud, “Microstereolithography : a new process to build complex 3D objects Fixed light spot,” vol. 3680, April, pp. 808–817, 1999.
- [10] C. Chatwin, M. Farsari, S. Huang, P. Birch, F. Claret-Tournier, R. Young, D. Budgett, and C. Bradfield, “Microfabrication by use of a spatial light modulator in the ultraviolet: experimental results.,” *Optics letters*, vol. 24, no. 8, pp. 549–50, Apr. 1999.
- [11] M. Farsari, F. Claret-Tournier, S. Huang, C. . Chatwin, D. . Budgett, P. . Birch, R. C. . Young, and J. . Richardson, “A novel high-accuracy microstereolithography method employing an adaptive electro-optic mask,” *Journal of Materials Processing Technology*, vol. 107, no. 1–3, pp. 167–172, Nov. 2000.
- [12] C. R. Chatwin, M. Farsari, S. Huang, M. I. Heywood, R. C. D. Young, P. M. Birch, F. Claret-Tournier, and J. D. Richardson, “Characterisation of Epoxy Resins for

- Microstereolithographic Rapid Prototyping,” *The International Journal of Advanced Manufacturing Technology*, vol. 15, no. 4, pp. 281–286, Apr. 1999.
- [13] C. Chatwin, M. Farsari, S. Huang, M. Heywood, P. Birch, R. Young, and J. Richardson, “UV Microstereolithography System that uses Spatial Light Modulator Technology.,” *Applied optics*, vol. 37, no. 32, pp. 7514–22, Nov. 1998.
- [14] S. Monneret, V. Loubère, S. Corbel, D. De Chimie, and B. P. N. Cedex, “Microstereolithography using a dynamic mask generator and a non-coherent visible light source,” vol. 3680, no. April, pp. 553–561, 1999.
- [15] A. Bertsch, “Microstereolithography: a Review,” in *Materials Research Society Symposium Proceedings*, 2002, vol. 758, p. 15.
- [16] C. B. Williams, F. Mistree, and D. W. Rosen, “A Functional Classification Framework for the Conceptual Design of Additive Manufacturing Technologies,” *Journal of Mechanical Design*, vol. 133, no. 12, p. 121002, 2011.
- [17] J.-W. Choi, R. Wicker, S.-H. Lee, K.-H. Choi, C.-S. Ha, and I. Chung, “Fabrication of 3D biocompatible/biodegradable micro-scaffolds using dynamic mask projection microstereolithography,” *Journal of Materials Processing Technology*, vol. 209, no. 15–16, pp. 5494–5503, Aug. 2009.
- [18] A. Bertsch, P. Bernhard, C. Vogt, and P. Renaud, “Rapid prototyping of small size objects,” *Rapid Prototyping Journal*, vol. 6, no. 4, pp. 259–266, 2000.
- [19] Y. Lu, G. Mapili, G. Suhali, S. Chen, and K. Roy, “A digital micro-mirror device-based system for the microfabrication of complex, spatially patterned tissue engineering scaffolds.,” *Journal of biomedical materials research. Part A*, vol. 77, no. 2, pp. 396–405, May 2006.
- [20] G. W. Hadipoespito, Y. Yang, H. Choi, G. Ning, and X. Li, “Digital Micromirror Device Based on Microstereolithography for Micro Structures of Transparent Photopolymer and Nanocomposites,” University of Wisconsin-Madison, Madison, Wisconsin, 2003.
- [21] L.-H. Han, G. Mapili, S. Chen, and K. Roy, “Projection Microfabrication of Three-Dimensional Scaffolds for Tissue Engineering,” *Journal Manufacturing Science and Engineering*, vol. Vol. 130, p. 021005: 1–4, 2008.
- [22] K. Takahashi and J. Setoyama, “A UV exposure system using DMD,” *Electronics and Communications in Japan (Part II: Electronics)*, vol. 83, no. 7, pp. 56–58, Jul. 2000.
- [23] A. Bertsch, P. Bernhard, and P. Renaud, “Microstereolithography : Concepts and applications,” vol. 00, pp. 289–298, 2001.

- [24] H.-W. Kang, J. H. Park, and D.-W. Cho, "A pixel based solidification model for projection based stereolithography technology," *Sensors and Actuators A: Physical*, vol. 178, pp. 223–229, May 2012.
- [25] J.-W. Choi, E. MacDonald, and R. Wicker, "Multi-material microstereolithography," *The International Journal of Advanced Manufacturing Technology*, vol. 49, no. 5–8, pp. 543–551, Dec. 2009.
- [26] Y. Chen, Y. Pan, and C. Zhou, "A Fast Mask Projection Stereolithography Process for Fabricating Digital Models in Minutes," *Journal of Manufacturing Science and Engineering*, vol. 134, no. 5, p. 051011, 2012.
- [27] T. V. Wilson, "How LCoS Works." [Online]. Available: <http://electronics.howstuffworks.com/lcos.htm>. [Accessed: 08-Jul-2013].
- [28] "3D Systems," 2013. [Online]. Available: <http://www.3dsystems.com/>. [Accessed: 08-Jul-2013].
- [29] A. S. Limaye and D. W. Rosen, "Compensation zone approach to avoid print-through errors in mask projection stereolithography builds," *Rapid Prototyping Journal*, vol. 12, no. 5, pp. 283–291, 2006.